

University of Dundee

**Inhibition of glycolysis and mitochondrial respiration promotes radiosensitisation of neuroblastoma and glioma cells**

Nile, Donna L.; Rae, Colin; Walker, David J.; Waddington, Joe Canning; Vincent, Isabel; Burgess, Karl

*Published in:*  
Cancer & Metabolism

*DOI:*  
[10.1186/s40170-021-00258-5](https://doi.org/10.1186/s40170-021-00258-5)

*Publication date:*  
2021

*Document Version*  
Publisher's PDF, also known as Version of record

[Link to publication in Discovery Research Portal](#)

*Citation for published version (APA):*

Nile, D. L., Rae, C., Walker, D. J., Waddington, J. C., Vincent, I., Burgess, K., Gaze, M. N., Mairs, R. J., & Chalmers, A. J. (2021). Inhibition of glycolysis and mitochondrial respiration promotes radiosensitisation of neuroblastoma and glioma cells. *Cancer & Metabolism*, 9, [24]. <https://doi.org/10.1186/s40170-021-00258-5>

**General rights**

Copyright and moral rights for the publications made accessible in Discovery Research Portal are retained by the authors and/or other copyright owners and it is a condition of accessing publications that users recognise and abide by the legal requirements associated with these rights.

- Users may download and print one copy of any publication from Discovery Research Portal for the purpose of private study or research.
- You may not further distribute the material or use it for any profit-making activity or commercial gain.
- You may freely distribute the URL identifying the publication in the public portal.

**Take down policy**

If you believe that this document breaches copyright please contact us providing details, and we will remove access to the work immediately and investigate your claim.

RESEARCH

Open Access



# Inhibition of glycolysis and mitochondrial respiration promotes radiosensitisation of neuroblastoma and glioma cells

Donna L. Nile<sup>1,2\*</sup> , Colin Rae<sup>1</sup>, David J. Walker<sup>1,3</sup>, Joe Canning Waddington<sup>1</sup>, Isabel Vincent<sup>4,5</sup>, Karl Burgess<sup>4,6</sup>, Mark N. Gaze<sup>7</sup>, Robert J. Mairs<sup>1</sup> and Anthony J. Chalmers<sup>1</sup>

## Abstract

**Background:** Neuroblastoma accounts for 7% of paediatric malignancies but is responsible for 15% of all childhood cancer deaths. Despite rigorous treatment involving chemotherapy, surgery, radiotherapy and immunotherapy, the 5-year overall survival rate of high-risk disease remains < 40%, highlighting the need for improved therapy. Since neuroblastoma cells exhibit aberrant metabolism, we determined whether their sensitivity to radiotherapy could be enhanced by drugs affecting cancer cell metabolism.

**Methods:** Using a panel of neuroblastoma and glioma cells, we determined the radiosensitising effects of inhibitors of glycolysis (2-DG) and mitochondrial function (metformin). Mechanisms underlying radiosensitisation were determined by metabolomic and bioenergetic profiling, flow cytometry and live cell imaging and by evaluating different treatment schedules.

**Results:** The radiosensitising effects of 2-DG were greatly enhanced by combination with the antidiabetic biguanide, metformin. Metabolomic analysis and cellular bioenergetic profiling revealed this combination to elicit severe disruption of key glycolytic and mitochondrial metabolites, causing significant reductions in ATP generation and enhancing radiosensitivity. Combination treatment induced G<sub>2</sub>/M arrest that persisted for at least 24 h post-irradiation, promoting apoptotic cell death in a large proportion of cells.

**Conclusion:** Our findings demonstrate that the radiosensitising effect of 2-DG was significantly enhanced by its combination with metformin. This clearly demonstrates that dual metabolic targeting has potential to improve clinical outcomes in children with high-risk neuroblastoma by overcoming radioresistance.

**Keywords:** Neuroblastoma, Radiation, Metabolism, 2-DG, Metformin, <sup>131</sup>I-MIBG

## Background

Neuroblastoma comprises 7% of paediatric malignancies but has a worse prognosis than many other tumour types, accounting for approximately 15% of childhood cancer deaths [1]. Age at diagnosis, along with stage and

molecular characteristics of the tumour, is used to allocate patients to low-intermediate- or high-risk groups. Younger age, low stage, and absence of segmental chromosomal abnormalities or oncogenic *MYCN* amplification are favourable features. However, most patients have high-risk disease by virtue of age greater than 12 months and distant metastatic disease or *MYCN* amplification [2]. The standard treatment schedule for high-risk neuroblastoma involves a complex multimodality schedule comprising induction chemotherapy [3],

\* Correspondence: [Donna.Nile@nhs.net](mailto:Donna.Nile@nhs.net)

<sup>1</sup>Institute of Cancer Sciences, University of Glasgow, Glasgow G61 1QH, UK

<sup>2</sup>Present Address: Integrated Covid Hub North East (ICHNE) Innovation Laboratory, Newcastle upon Tyne Hospitals NHS Foundation Trust, Newcastle upon Tyne NE4 5BX, UK

Full list of author information is available at the end of the article



© The Author(s). 2021 **Open Access** This article is licensed under a Creative Commons Attribution 4.0 International License, which permits use, sharing, adaptation, distribution and reproduction in any medium or format, as long as you give appropriate credit to the original author(s) and the source, provide a link to the Creative Commons licence, and indicate if changes were made. The images or other third party material in this article are included in the article's Creative Commons licence, unless indicated otherwise in a credit line to the material. If material is not included in the article's Creative Commons licence and your intended use is not permitted by statutory regulation or exceeds the permitted use, you will need to obtain permission directly from the copyright holder. To view a copy of this licence, visit <http://creativecommons.org/licenses/by/4.0/>. The Creative Commons Public Domain Dedication waiver (<http://creativecommons.org/publicdomain/zero/1.0/>) applies to the data made available in this article, unless otherwise stated in a credit line to the data.

surgery [4], high-dose chemotherapy [5], radiotherapy [6] and immunotherapy [7]. While some patients respond well, some are refractory to initial treatments or relapse later. As neuroblastoma arises from primordial neural crest cells, most commonly in the adrenal medulla and also at other sites in the sympathetic nervous system, neuroblastoma cells usually retain the ability to take up catecholamines and analogues such as metaiodobenzylguanidine (MIBG) [8]. Imaging with  $^{123}\text{I}$ -MIBG is used for staging and response assessment, and  $^{131}\text{I}$ -MIBG is a valuable treatment option [9].

The prognosis for patients with high-risk neuroblastoma has undoubtedly improved significantly over recent decades due to international cooperative group phase III trials investigating intensification of treatments such as high-dose chemotherapy and immunotherapy. Different sources yield different survival rates depending on the era of presentation, clinical trial selection factors, treatments used, and follow-up duration. Ten-year overall survival rates remain in the order of only 40% [10, 11], and while newer approaches offer the prospect of improvements in long-term survival, follow-up durations are currently insufficient to confirm these hopes [12]. Although  $^{131}\text{I}$ -MIBG is useful in the treatment of refractory and relapsed high-risk neuroblastoma and is the subject of clinical trials ([ClinicalTrials.gov](https://clinicaltrials.gov) identifiers NCT02035137 and NCT03165292) aiming to optimise its use, further strategies are required to ensure that maximal benefit is obtained [13, 14]. It is likely that maximal therapeutic benefit from targeted radiotherapy will be obtained by its combination with drugs [14], which might render it more effective specifically for high-risk neuroblastoma patients, who do not benefit from existing therapies.

In recent years, a growing body of evidence has emerged demonstrating the anticancer properties of drugs that modulate cellular metabolism. Aberrant mitochondrial metabolism is a common trait among cancers. This is exemplified by the Warburg effect, which is characterised by increased rates of glycolysis and lactate production, even in the presence of oxygen [15]. Dysregulated cancer cell metabolism has been linked to increased tumour aggressiveness and treatment resistance [16]. Indeed, targeting glucose metabolism has yielded chemo- and radiosensitisation in several cancer types [17, 18]. Of relevance to this study, neuroblastoma cells have been reported to exhibit aberrant metabolic properties, including increased fatty acid synthase expression [19] and altered fatty acid and glucose metabolism [20].

The synthetic glucose analogue 2-deoxyglucose (2-DG) is avidly taken up by rapidly proliferating cells, including cancer cells. Once internalised, 2-DG is unable to undergo isomerisation at its second carbon atom to produce 2-deoxyglucose-6-phosphate, a phenomenon that leads to

inhibition of glycolysis at the phosphoglucosomerase level. Therefore, treatment with 2-DG becomes cytotoxic in the contexts of ATP depletion [21] or disruption of glutathione metabolism [22]. In keeping with this, 2-DG was shown to be an effective radiosensitiser of HeLa cells [22] and was well tolerated in combination with docetaxel in a phase 1, dose-escalation clinical trial [23].

Metformin is a biguanide drug that is widely prescribed for the treatment of type 2 diabetes, acting to reduce insulin resistance, enhance glucose utilisation and reduce hepatic glucose production [24]. At the cellular level, metformin promotes AMPK activation during energy homeostasis via inhibition of Complex I of the mitochondrial respiratory chain [25, 26]. Indeed, metformin has been shown to exhibit antineoplastic activity in the context of exogenously induced changes in energy homeostasis [27]. Additionally, patients with type 2 diabetes who were receiving metformin as part of their diabetic management have been shown to experience reduced incidence and better survival rates for many solid cancers [28–30].

In keeping with these observations, both 2-DG and metformin have shown potential as radio- [22, 31–34] and chemosensitisers [23, 35, 36]. However, their ability to sensitise neuroblastoma cells to radiotherapy has not yet been studied, and the mechanisms underlying their radiosensitising properties are poorly understood. Accordingly, we investigated the potential of 2-DG and metformin to enhance the efficacy of X-irradiation in pre-clinical models of neuroblastoma. We show that 2-DG effectively radiosensitises neuroblastoma and glioma cells, effects that are significantly enhanced in the presence of metformin, and demonstrate that combining 2-DG, metformin and radiation induces extensive metabolic reprogramming. This is characterised by reduced cellular respiration and ATP production that associates with prolonged  $G_2/M$  arrest during which cells ultimately succumb to apoptotic cell death. Our results indicate that dual pharmacological inhibition of glycolysis and mitochondrial respiration has potential to enhance the efficacy of radiation therapy in patients with neuroblastoma.

## Materials and methods

### Reagents

2-Deoxy-D-glucose (2DG; D3179) and metformin hydrochloride (PHR1084) were purchased from Sigma-Aldrich (Poole, UK) and were reconstituted using sterile water. Drugs were then diluted in culture medium. Unless otherwise stated, all other cell culture reagents were purchased from Thermo Fisher Scientific (Paisley, UK) and all chemicals were purchased from Sigma-Aldrich (Poole, UK).

### Cell culture

Human neuroblastoma SK-N-BE(2c) cells were purchased from the American Type Culture Collection and were maintained in Dulbecco's modified Eagle medium (DMEM) containing 15% (v/v) fetal calf serum, 2 mM L-glutamine and 1% (v/v) non-essential amino acids. Human glioblastoma UYW cells were transfected with a plasmid containing the bovine noradrenaline transporter (NAT) gene [37] and were maintained in minimum essential medium (MEM) containing 10% (v/v) fetal calf serum, 2 mM L-glutamine, 1% (v/v) non-essential amino acids and 1 mg/ml geneticin. Human neuroblastoma CHLA-20 cells were obtained from the Children's Oncology Group Childhood Cancer Repository (TX, USA) and were maintained in Iscove's modified Dulbecco's medium (IMDM) containing 20% (v/v) fetal calf serum, 2 mM L-glutamine and 1% (v/v) insulin-transferrin-selenium. All cells were incubated at 37 °C, 5% CO<sub>2</sub> in a humidified incubator, and were passaged every 3–4 days. Cell lines were cultured in this study for less than 6 months after resuscitation and were deemed free of Mycoplasma contamination by in-house testing using the MycoAlert mycoplasma detection kit (Lonza, Bazel, Switzerland).

### MTT cell growth assay

The MTT reduction assay was used to estimate the effect of drug treatment on cell growth up to 96 h post treatment. After seeding cells in 96-well plates, the following day, cells were washed with PBS before adding 200 µl drug-containing medium. After 24 h, 48 h, 72 h, and 96 h, cells were incubated for 2 h with 20 µl MTT solution (5 mg/ml MTT in PBS). Internalised MTT was solubilised with DMSO and absorbance was measured at 570 nm.

### Clonogenic assay

Monolayers were cultured in 25 cm<sup>2</sup> flasks before 24-h drug treatment and simultaneous irradiation (Xstrahl RS225 X-Ray irradiator, Xstrahl Limited, Surrey, UK; dose rate of 0.93 Gy/min) at the stated concentrations and doses. Irradiation was always administered at the beginning of drug treatment, with the only exception being during the alternative scheduling experiments (as further detailed in the text). Clonogenic survival was determined by seeding 500 (SK-N-BE(2c)) or 250 (UYW/NAT) cells in to 21.5 cm<sup>2</sup> petri dishes as previously described [38].

### Spheroid growth delay

Cells were cultured in 25 cm<sup>2</sup> flasks coated with 1% (w/v) agar to initiate multicellular spheroid formation. After 3 days, spheroids were transferred to sterile universal tubes before treatment in serum-free drug-containing medium and simultaneous irradiation. Spheroids were treated for 24 h, and those of approximately 100 µm in

diameter were individually transferred to agar-coated 24-well plates, with 12 replicate spheroids per condition, as previously described [39, 40]. Each spheroid was imaged every 3–4 days for 3 weeks using an inverted phase contrast microscope. The longest spheroid length,  $d_{\max}$ , and its perpendicular width,  $d_{\min}$ , were measured using ImageJ (NIH, Bethesda, MD). Tumour volume,  $V$  (µm<sup>3</sup>) was then estimated assuming  $V = \pi \times d_{\max} \times d_{\min}^2/6$  [41], which allowed determination of the area under the  $V/V_0$  versus time curve (AUC) using trapezoidal approximation [39, 40].

### Untargeted metabolomic analysis

Hydrophilic interaction liquid chromatography (HILIC) was carried out on a Dionex UltiMate 3000 RSLC system (Thermo Fisher Scientific, Hemel Hempstead, UK) using a ZIC-pHILIC column (150 mm × 4.6 mm, 5-µm column, Merck Sequant). The column was maintained at 30 °C and samples were eluted with a linear gradient (20 mM ammonium carbonate in water and acetonitrile) over 26 min at a flow rate of 0.3 ml/min. The injection volume was 10 µl and samples were maintained at 5 °C prior to injection. Metabolites were detected using the Thermo Orbitrap Q Exactive (Thermo Fisher Scientific) mass spectrometer at a resolution of 70,000 (at 70–1050 m/z), which was operated in polarity switching mode. A pooled sample comprising a mixture of all sample extracts was analysed using the same conditions and was run every 5th sample. Instrument .raw files were converted to positive and negative ionisation mode mzXML files. These files were then analysed using the XCMS [42]/MZMatch [43]/IDEOM pipeline. Polyomics integrated Metabolomics Pipeline (PiMP) and FrAnK were used to assess fragmentation data [44]. The weighted distance of treatment conditions to untreated control samples was calculated using the following equation:

$$\text{Weighted distance} = \sqrt{((PC1_{rep_n} - PC1_{Ctrl_{mean}}) \times 0.49)^2 + ((PC2_{rep_n} - PC1_{Ctrl_{mean}}) \times 0.218)^2}$$

where  $PC1_{rep_n}$  is the PC1 value of each replicate and  $PC1_{Ctrl_{mean}}$  is the mean PC1 value of all untreated control samples [45]. All metabolomic data has been uploaded to the repository MetaboLights (<https://www.ebi.ac.uk/metabolights/>).

### Bioenergetic analysis of glycolysis and mitochondrial respiration

UYW/NAT cells and CHLA-20 cells were seeded at a density of  $1 \times 10^4$  and  $3 \times 10^4$  cells, respectively, in a volume of 175 µl in Seahorse XFe96-well plates (Cat# 101085-004, Seahorse Biosciences, Agilent Technologies, Cheshire, UK). Cells were allowed to settle for 2 h at room temperature, before drug treatment (25 µl) and simultaneous irradiation, as required. Mitochondrial

respiration was measured 24 h after treatment using the Seahorse XFe96 Analyzer (Seahorse Biosciences, Agilent Technologies, Cheshire, UK) according to manufacturer's instructions. On the day of the assay, culture medium was replaced with Seahorse XF base medium (Cat# 102353-100), supplemented with the reagents required for each cell line (except FBS), as detailed above. Cells were then incubated for 1 h at 37 °C in the absence of CO<sub>2</sub>. Using the Seahorse Cell Mito Stress Test (Cat# 103015-100), sequential injections were made of oligomycin (1 μM), carbonyl cyanide-p-trifluoromethoxyphenylhydrazone (FCCP) (1 μM), rotenone (0.5 μM) and antimycin A (0.5 μM) to test cellular response to mitochondrial stress in live cells. Mitochondrial oxygen consumption rate (OCR) and extracellular acidification rate (ECAR) were measured every 3 min, for a total of 75 min. The OCR and ECAR traces were then used to estimate basal and maximal respiration, ATP synthesis, and glycolytic rate as described previously [46]. Data were normalised to protein content, which was determined after each Seahorse assay using the Pierce Micro BCA Protein Assay kit (Cat# 23235, Thermo Fisher Scientific, Paisley, UK), following manufacturer's instructions.

#### Fluorescence-activated cell sorting (FACS) analysis

Cells were seeded at a density of  $7 \times 10^5$  (SK-N-BE(2c)) or  $4 \times 10^5$  (UVW/NAT) cells in 75 cm<sup>2</sup> flasks. Drug-containing medium was added once cells were 60% confluent, and cells were simultaneously irradiated. After 24 h, cells were trypsinised and washed with PBS, before fixing with 70% (v/v) ethanol in water at -20°C for a minimum of 6 h. Ethanol was removed by washing with PBS and cells were resuspended in PBS containing propidium iodide (10 μg/ml) and RNase A (200 μg/ml), before analysis using a BD FACSVerser flow cytometer (BD BioSciences, Oxford, UK). FACS data were quantified using FlowJo 7.6.5 software. Our gating strategy is provided in Supplementary Information Fig. S8a.

#### Live cell imaging

For real-time analysis of cellular proliferation and apoptotic frequency, UUVW/NAT and CHLA20 cells were seeded in 96-well plates at densities of  $1.5 \times 10^3$  or  $1.75 \times 10^4$  cells/well, respectively. After overnight incubation at 37 °C, Annexin V-labelled cells (IncuCyte Annexin V Red, Cat# 4641, Essen BioScience, 1:400) were analysed with the IncuCyte ZOOM live cell imaging system (Essen BioScience, Hertfordshire, UK) following drug treatment (as detailed in the text). Each condition was replicated in six wells per experiment for each cell line. Two images per well were acquired every hour at a magnification of  $\times 10$ , over a time period of 50 h. The number of Annexin V-positive cells was normalised to total cell confluence, using the IncuCyte ZOOM 2018A software (Ann Arbor, MI, USA).

## Results

### Radiosensitising effect of 2-DG and metformin as single agents

Both 2-DG and metformin exhibited modest activity as single agents, with reductions in cell proliferation and clonogenic survival being observed after exposure to concentrations greater than 1 mM 2-DG or 10 mM metformin (Supplementary Information Fig. S1a-d). When delivered for 24 h commencing at the time of external beam radiation, 2-DG reduced the clonogenic capacity of UUVW/NAT cells in a dose-dependent manner, with statistically significant radiosensitisation observed at 5 mM and 10 mM, with dose enhancement factors at 50% cell kill (DER<sub>50</sub>) of 1.80 and 1.69, respectively (Fig. 1a). Similarly, 10 mM 2-DG significantly enhanced X-irradiation induced growth delay in SK-N-BE(2c)-derived spheroids, with the combined effect being greater than either agent administered alone (Fig. 1b). In contrast, metformin had negligible effect on clonogenic survival of UUVW/NAT cells when administered in combination with irradiation (Fig. 1c), results that were confirmed in SK-N-BE(2c) cells (Supplementary Information Fig. S2).

### Combined effects of 2-DG and metformin on radiosensitisation

The failure of metformin to radiosensitise neuroblastoma and glioma cells contrasts with data from previous studies on pancreatic [31] and breast cancer cells [34]. However, there is a rationale for combining metformin treatment with 2-DG treatment. Inhibition of glycolysis by 2-DG is predicted to cause a compensatory increase in mitochondrial respiration to maintain ATP production. Combination treatment with metformin would circumvent this compensatory increase in mitochondrial metabolism by inhibiting Complex 1 of the respiratory chain. There is also evidence of supra-additive activity of 2-DG and metformin combination treatment in other cancer types [47–49]. Most pertinently, Chatterjee and colleagues demonstrated that simultaneous administration of 2-DG and metformin enhanced radiation-induced cytotoxicity in two breast cancer cell lines [50].

In keeping with this rationale, 2-DG and metformin exerted additive effects on clonogenic cell kill in the absence of radiation (Supplementary Information Fig. S1e-f). Likewise, dual treatment with low doses of 2-DG and metformin (1 mM) significantly radiosensitised UUVW/NAT cells (drugs administered for 24 h commencing at the time of irradiation, Fig. 2a) but failed to radiosensitise SK-N-BE(2c) cells (Fig. 2b).

Since SK-N-BE(2c) cells exhibit a longer population doubling time (37 h) than UUVW/NAT cells (16 h), we postulated that more prolonged drug treatment might be required to radiosensitise these cells. However, 48h

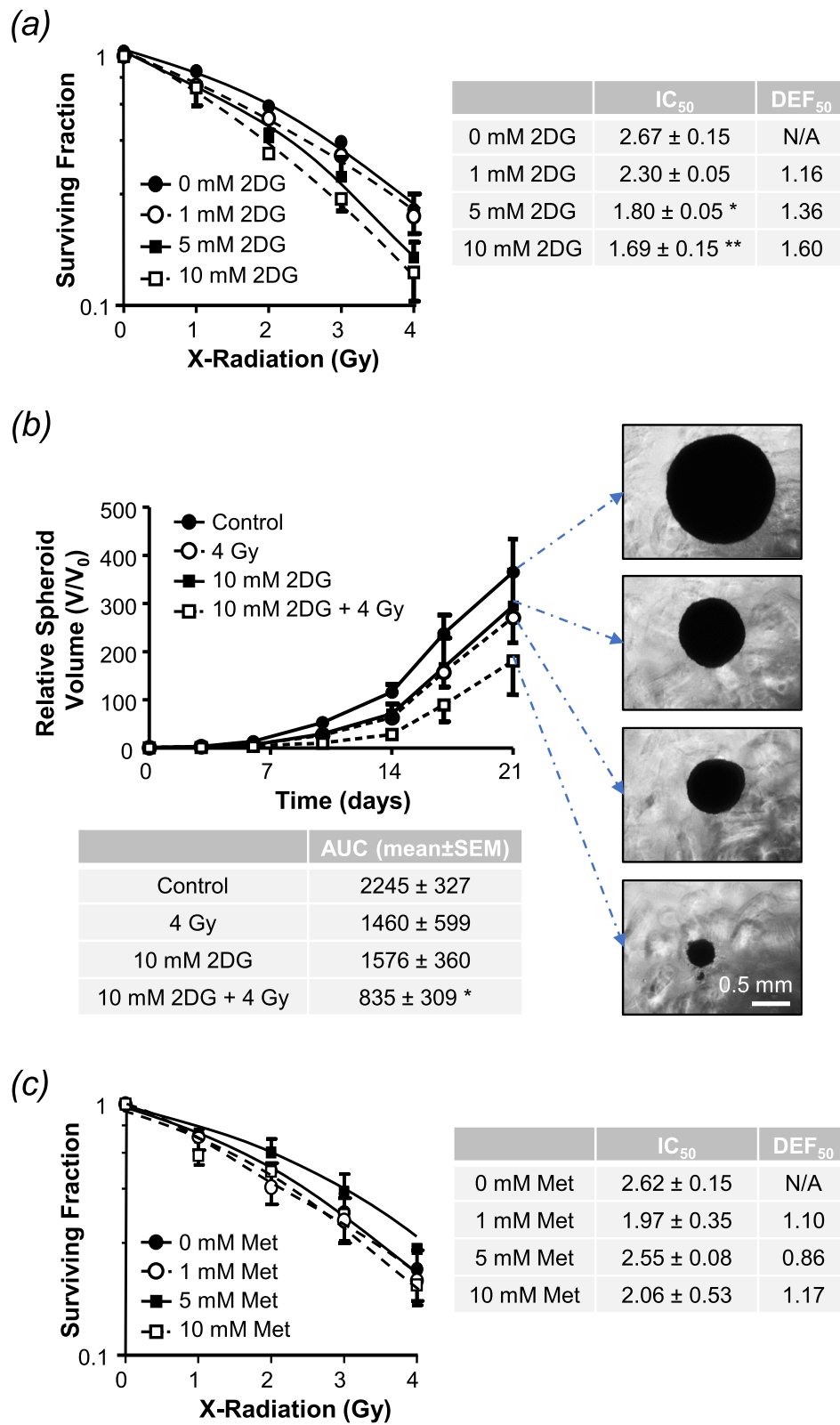


Fig. 1 (See legend on next page.)

(See figure on previous page.)

**Fig. 1** Radiosensitising effect of 2DG and metformin as single agents. The clonogenic survival of UVW/NAT cells following 24-h treatment with **a** 1, 5, or 10 mM 2DG or **c** 1, 5, or 10 mM metformin in the presence 1–4 Gy X-radiation (administered at the beginning of drug treatment). The 50% inhibitory concentration ( $IC_{50}$ ) and the dose enhancement factor observed at the 50% kill level ( $DEF_{50}$ ) are shown. **b** Growth inhibition of SK-N-BE(2c)-derived multicellular spheroids ( $n = 3$ ) after 24-h treatment with 4 Gy X-radiation or 10 mM 2DG, as single agents or in combination. Data expressed as percentage are under the volume-time curve (AUC) with representative spheroids shown after 21-day treatment,  $\times 5$  magnification.  $*p < 0.05$ ,  $**p < 0.01$  compared to untreated control cells. All data are mean  $\pm$  SEM from 3 experimental repeats

exposure to metformin and 2-DG also failed to increase radiation-induced cell kill (Fig. 2b).

Because of the discrepancy between UVW/NAT glioma cells and SK-N-BE(2c) neuroblastoma cells, we evaluated an alternative human neuroblastoma cell line, CHLA-20. These cells were unable to form the colonies required for clonogenic assay but readily formed three-dimensional spheroids. In this clinically relevant model, we observed

enhanced spheroid growth delay following triple combination therapy, as opposed to single agent modalities (Fig. 2c).

**Combination treatment significantly disrupts glycolysis, mitochondrial respiration and nucleotide metabolism**

To understand why metformin enhanced the radiosensitising potential of 2-DG in UVW/NAT cells, we

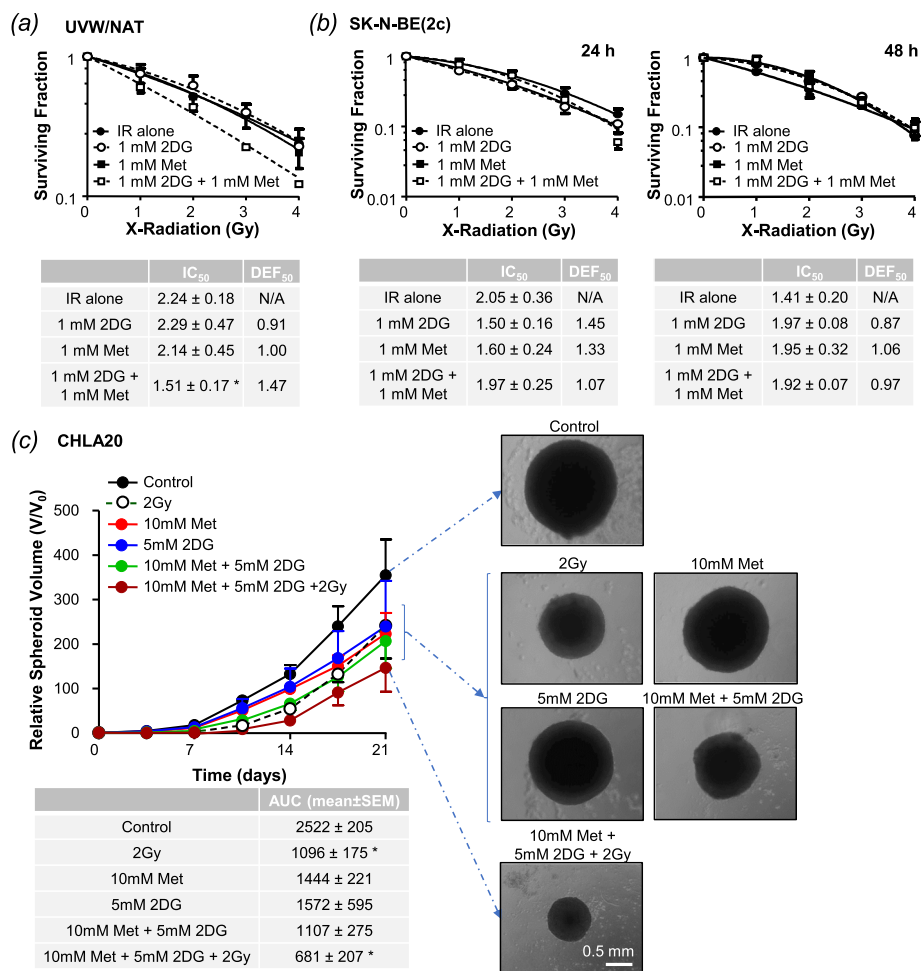


**Fig. 2** Combined effect of 2DG and metformin on radiosensitisation. The effect of 2DG and metformin on the radiation-induced cell kill of **a** UVW/NAT ( $n = 3$ ) cells after 24h drug treatment and **b** SK-N-BE(2c) cells after 24h ( $n = 4$ ) or 48h ( $n = 2$ ) drug treatment. **c** Growth inhibition of CHLA20-derived multicellular spheroids ( $n = 3$ ) after 24h treatment with 2 Gy X-radiation (at the beginning of treatment), 10 mM metformin, or 5 mM 2DG, as single agents or in combination. Data expressed as percentage are under the volume-time curve (AUC). Representative CHLA20-derived spheroids are shown after 21-day treatment,  $\times 5$  magnification. Data are means  $\pm$  SEM from the stated number of experimental repeats.  $*p < 0.05$ ,  $**p < 0.01$ ,  $***p < 0.001$  compared to irradiated (IR) cells (**a, b**) or untreated control cells (**c**)

interrogated the effect of single agent and combination treatments on glycolytic and mitochondrial respiration metabolites. An initial untargeted analysis using a principal component plot revealed that 2-DG induced significant changes in the metabolomic composition of UVW/NAT cells, whether administered as a single agent or in combination (Fig. 3a). Further interrogation of glycolytic pathway metabolites revealed 2-deoxyglucose phosphate to be significantly increased in cells exposed to 2-DG treatment, proving that 2-DG was internalised and phosphorylated by hexokinase (Fig. 3b). This phosphorylation rendered 2-DG refractory to metabolism by glycolysis, as shown by the reduction in glyceraldehyde-3-phosphate, phosphoenolpyruvate and pyruvate, the end-product of glycolysis, in all treatments involving 2-DG (Fig. 3b and Supplementary Information Fig. S3a).

Likewise, investigation of the tricarboxylic acid (TCA) cycle (Supplementary Information Fig. S3c) revealed citrate/isocitrate and malate to be significantly reduced following exposure to single agent or combination therapy involving 2-DG (Fig. 3c). Single agent metformin treatment also significantly reduced the relative abundances of these metabolites, demonstrating inhibition of Complex 1 of the respiratory chain.

Our metabolomic analysis also revealed that 2-DG single agent treatment promoted large-scale changes in purine and pyrimidine metabolism. Specifically, we observed a decreased abundance in 20 of 26 metabolites detectable within the purine metabolic pathway (Supplementary Information Fig. S4). Similarly, 2-DG promoted a reduction in 11 of the 27 metabolites we detected within the pyrimidine metabolic pathway (Supplementary Information Fig. S5). Comparable results were observed after metformin single agent therapy, but to a lesser extent (data not shown). Further analysis of combination treatments revealed that dual 2-DG/metformin and triple 2-DG/metformin/radiation combination therapies significantly increased the abundance of ethanolamine phosphate and hypoxanthine (Fig. 3d;  $p < 0.001$ ), which are products of serine and adenine metabolism, respectively. Interestingly, the increased abundance of these two metabolites was only observed following combination treatments.

#### **Metabolite imbalance following therapeutic intervention culminates in impaired cellular respiration**

Having demonstrated marked disruption of glycolysis and mitochondrial metabolism by our combination drug treatment, we explored its effects on cellular respiration and energy production. The mitochondrial respiratory profile of UVW/NAT and CHLA-20 cells was analysed using the Seahorse XF system, whereby live cells were sequentially injected with different test compounds to induce mitochondrial stress (Supplementary Fig. S6).

Initially, basal extracellular acidification rate (ECAR) was plotted against mitochondrial oxygen consumption rate (OCR) (Fig. 4a). While these bioenergetic profiles were unaffected by irradiation (3 Gy), 2-DG treatment promoted aerobic respiration, presumably in response to glycolytic inhibition, whereas metformin-treated cells became increasingly glycolytic as mitochondrial respiration was inhibited (Fig. 4a, b). The greatest shift in bioenergetics was seen following combination therapy involving 2-DG and metformin in the presence or absence of radiation, with cells becoming less energetic and more quiescent as the two central ATP production pathways were inhibited. Interestingly, single agent metformin produced the greatest shift in mitochondrial respiratory capacity, with no additional effect observed when 2-DG or radiation were added (Fig. 4c). Single agent 2-DG treatment, however, significantly increased both the respiratory capacity and ATP production of UVW/NAT cells. Our hypothesis that this reflected increased utilisation of more efficient mitochondrial ATP production was supported by the reversal of the effect that was observed when metformin was added (with or without irradiation, Fig. 4c, d). Comparably, combination treatment significantly reduced abundance of the metabolites AMP, ADP and ATP (Supplementary Information Fig. S3d). Similar results were obtained in CHLA-20 cells (Supplementary Fig. 7).

Taken together, these results demonstrate that 2-DG and metformin treatment caused significant disruption of glycolysis and/or the mitochondrial TCA cycle, which culminated in significantly impaired cellular energy production. However, this effect was not enhanced in the presence of irradiation, even though both drugs were required to enhance radiosensitivity.

#### **Triple combination therapy significantly prolongs G<sub>2</sub>/M cell cycle arrest**

To further understand the mechanisms underlying the efficacy of triple combination therapy, effects on cell cycle progression were investigated using the gating strategy presented in Supplementary Fig. S8a. Single agent 2-DG treatment at doses of 2.5 mM and above caused accumulation of cells in G<sub>2</sub>/M phase of the cell cycle after 6 h, whereas metformin had negligible effect on the proportion of G<sub>2</sub>/M phase cells at any dose (Supplementary Fig. S8b-c). However, combined low-dose (1 mM) treatment with 2-DG and metformin caused a marked G<sub>2</sub>/M arrest that was observed 6 h after treatment and failed to resolve at 24 h (Fig. 5a). Radiation alone (3 Gy) caused a temporary G<sub>2</sub>/M arrest, as expected, but did not amplify cell cycle effects of the drug combination (Fig. 5a).

Our previous studies have demonstrated the importance of scheduling when combining treatment modalities [39, 51], and we predicted that accumulation of cells in G<sub>2</sub>/M phase of the cell cycle would increase radiosensitivity [52] by doubling the amount of DNA



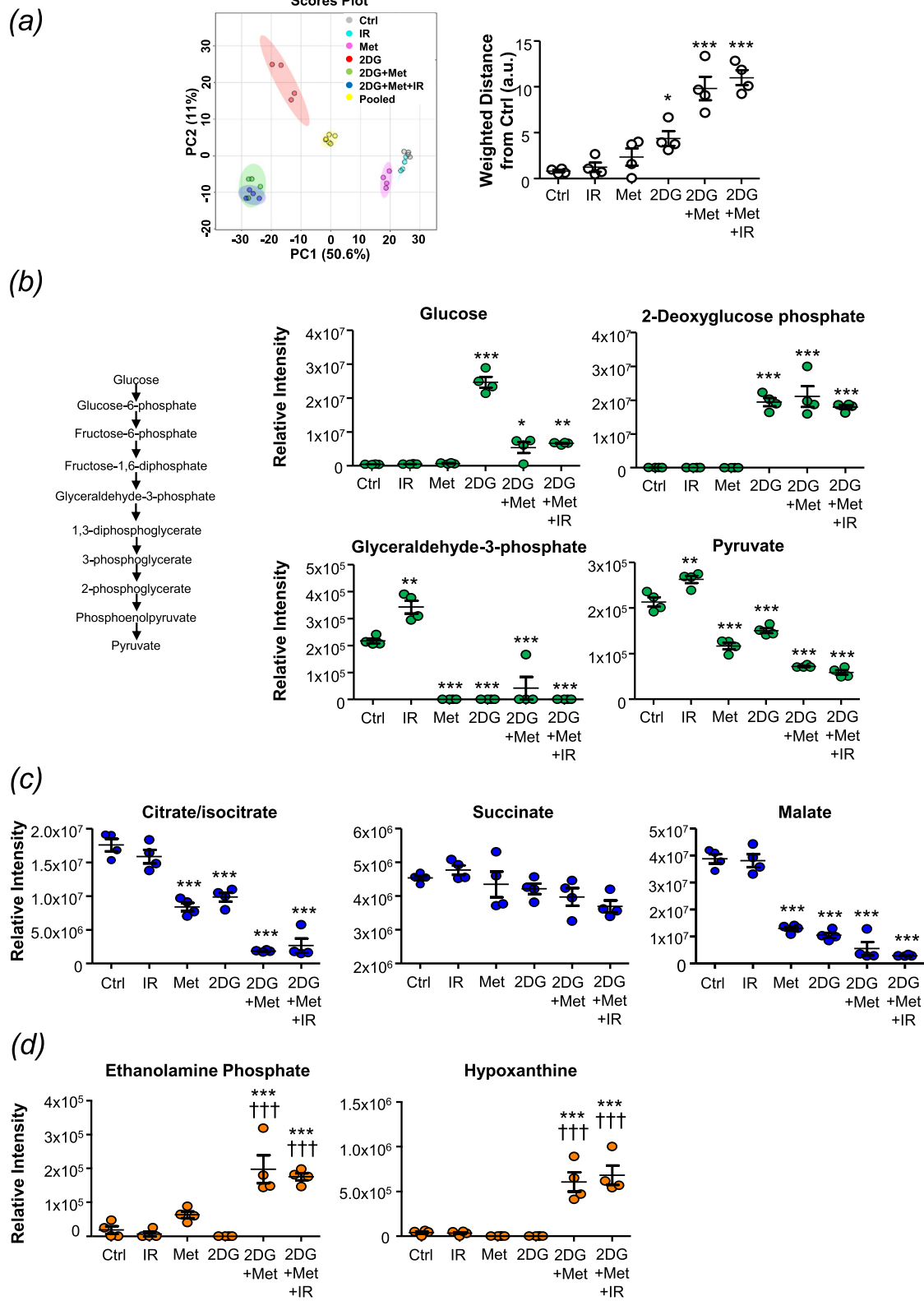


**Fig. 3** (See legend on next page.)

(See figure on previous page.)

**Fig. 3** Effect of combination treatment on glycolytic and mitochondrial metabolites. UWW/NAT cells were treated with 3 Gy X-radiation, 1 mM metformin, or 2.5 mM 2DG as single agents or in triple combination for 24 h. Cells were then harvested in solvent extraction buffer and analysed by mass spectrometry in quadruplicate. **a** Principal component analysis (PCA) plot showing biological variation within the data set, which was then used to calculate the weighted distance between each culture condition and their respective mean values  $\pm$  SD. Intracellular relative intensity of **b** glycolytic intermediates (including a schematic representation of the glycolytic pathway), **c** tricarboxylic acid (TCA) cycle metabolites and **d** by-products of purine and pyrimidine metabolism. Data are means  $\pm$  SD,  $n = 4$ . Treatment vs control: \* $p < 0.05$ , \*\* $p < 0.01$ , \*\*\* $p < 0.001$ ; treatment vs 2-DG:  $^{+++}p < 0.0001$  following a one-way ANOVA with Bonferroni correction

susceptible to radiation damage in each cell. To investigate this possibility, three different schedules were tested: (1) three treatments simultaneously, (2) 2-DG and metformin 6 h prior to irradiation, and (3) irradiation 6 h prior to 2-DG and metformin (Supplementary Fig. S8d). Cells were harvested after a total treatment time of 24 h and analysed by propidium iodide staining and flow cytometry (Fig. 5b) or clonogenic assay (Fig. 5c), to determine effects on cell cycle distribution and cell survival, respectively. The 6h interval was selected because maximum  $G_2/M$  arrest was observed at this timepoint (Fig. 5a) [38].

Maximum  $G_2/M$  arrest at 24 h was observed when cells were irradiated 6 h prior to drug therapy (Schedule 3, Fig. 5b). Schedules 1 and 2 were less effective, yielding

2-fold increases in the proportion of cells in  $G_2/M$  phase. While all three combination schedules enhanced clonogenic cell kill compared to individual treatments (Fig. 5c), no difference in efficacy was observed between the different schedules. These results demonstrate that increased  $G_2/M$  arrest does not necessarily translate into increased clonogenic cell kill for this combination.

#### Sustained $G_2/M$ arrest promotes apoptotic cell death

To interrogate the possibility that prolonged  $G_2/M$  arrest following triple combination therapy would culminate in apoptotic cell death, we used IncuCyte live cell imaging to determine the proportion of cells expressing the apoptotic marker Annexin V at multiple timepoints after treatments.

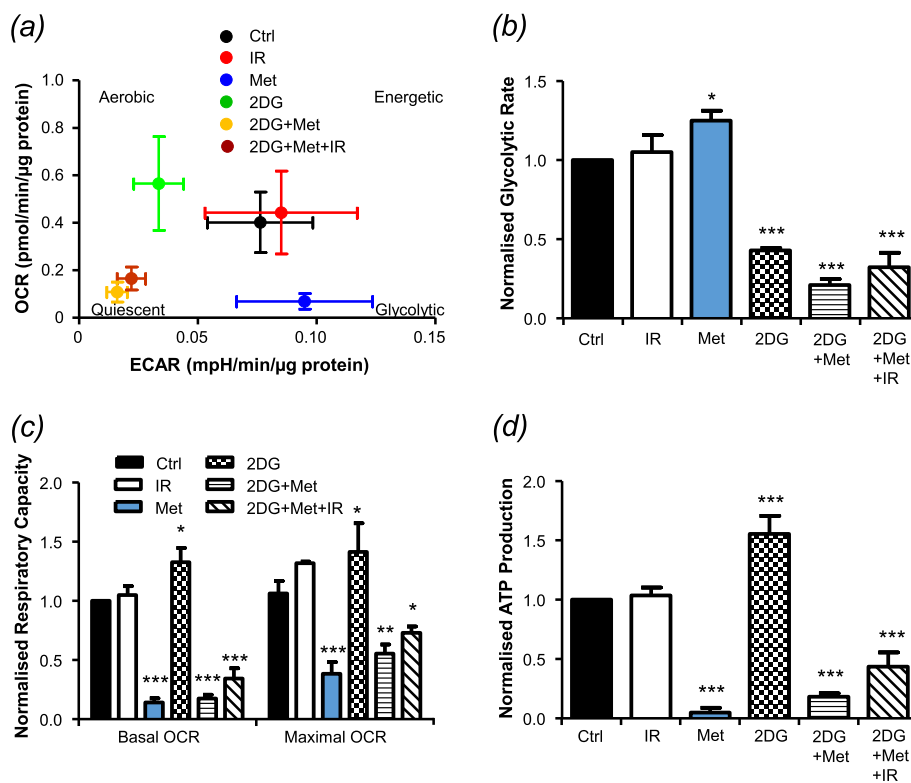


**Fig. 4** The effect of combination treatment on mitochondrial respiration, glycolysis and cellular energy production. UWW/NAT cells were treated with 3 Gy X-radiation, 1 mM metformin, or 5 mM 2DG as single agents or in combination for 24 h. Oxygen consumption rate (OCR) and extracellular acidification rate (ECAR) of live cells were then measured using a Seahorse XFe96 Analyser, the shift in cell energy phenotype following treatment is shown (a) The traces obtained (Supplementary Figure 6) were then used to calculate glycolytic rate (b), minimal and maximal respiratory capacity (c) and ATP production (d)

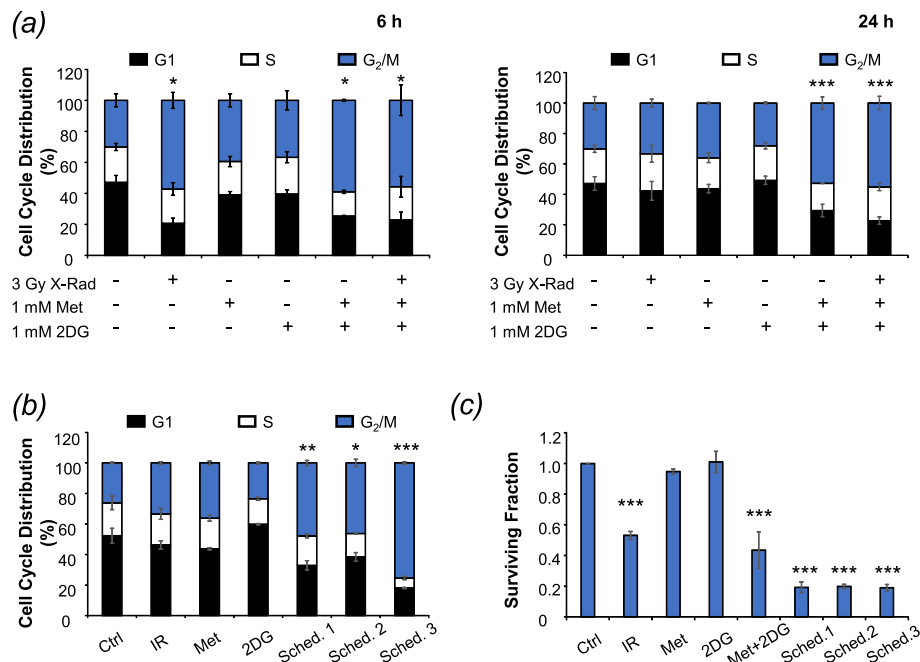


**Fig. 5** The effect of 2DG and metformin on the cell cycle and alternative scheduling. **a** UWW/NAT cells were treated with 3 Gy X-radiation, 1 mM metformin, or 1 mM 2-DG, as single agents or in simultaneous combination for 6 h or 24 h, and cell cycle distribution was determined following propidium iodide staining and flow cytometric analysis. The effect of scheduling on **b** the cell cycle and **c** clonogenic survival ( $n = 4$ ). Data presented are means  $\pm$  SEM from 3 independent experiments, unless otherwise stated. \* $p < 0.05$ , \*\* $p < 0.01$ , \*\*\* $p < 0.001$  compared to untreated control cells

These data showed that 2-DG but not metformin caused modest levels of apoptotic cell death as a single agent, with dual drug therapy showing a supra-additive effect in UVW/NAT cells (Fig. 6a, c). Radiation alone induced moderate apoptosis at early timepoints but did not further enhance efficacy of the 2-DG/metformin combination (Fig. 6b, c). Similar results were observed using CHLA-20 cells (Supplementary Fig. S9).

## Discussion

Despite rigorous multi-modal treatment regimens involving surgical resection, chemotherapy, radiotherapy and immunotherapy, high-risk neuroblastoma patients have 10-year overall survival rates of less than 40% [10, 11]. Targeted radiotherapy remains one of the most effective treatment options for high-risk disease [53], but most patients are not cured and so there is scope to improve its efficacy by using targeted drugs to overcome treatment resistance [14].

In this study we aimed to enhance radiosensitivity by inhibiting glycolysis, which is upregulated in cancer cells, thus disrupting the ATP generation required to fuel their rapid proliferation. Anticipating a compensatory increase in mitochondrial metabolism to maintain ATP production, we hypothesised that this could be circumvented by adding the mitochondrial respiratory chain inhibitor metformin. Building on recent observations in breast cancer cells [50],

we tested these hypotheses by measuring the effects of 2-DG and metformin on the radiation responses of neuroblastoma and glioma cells.

Metformin failed to radiosensitise neuroblastoma (SK-N-BE(2c)) or glioma (UVW/NAT) cells when administered as a single agent, which is contrary to previous reports [31, 32, 34]. However, we did observe that low-dose 2-DG and metformin given in combination significantly increased the radiosensitivity of UVW/NAT cells but had negligible effects on SK-N-BE(2c) neuroblastoma cells, even when treatment was extended to 48 h. These observations are consistent with previous reports demonstrating a range of sensitivities to 2-DG and metformin combination treatment across cell lines [47–49]. Variability in response to metformin has been attributed to genetic characteristics including p53 deficiency [47, 48], AMPK $\alpha$  expression [34] and MYC status [49, 54].

Resistance of SK-N-BE(2c) cells to the 2-DG/metformin combination is likely to be explained by their genetic background, which includes p53 mutations [55] and amplification of the *MYCN* gene [56]. Amplification of the neuronal transcription factor MYCN induces malignant transformation of neuroblastoma cells and is used for disease stratification [57], and sensitivity of neuroblastoma cells to impaired polyamine metabolism has been demonstrated to correlate with extent of *MYCN* amplification [54]. We therefore extended our study to

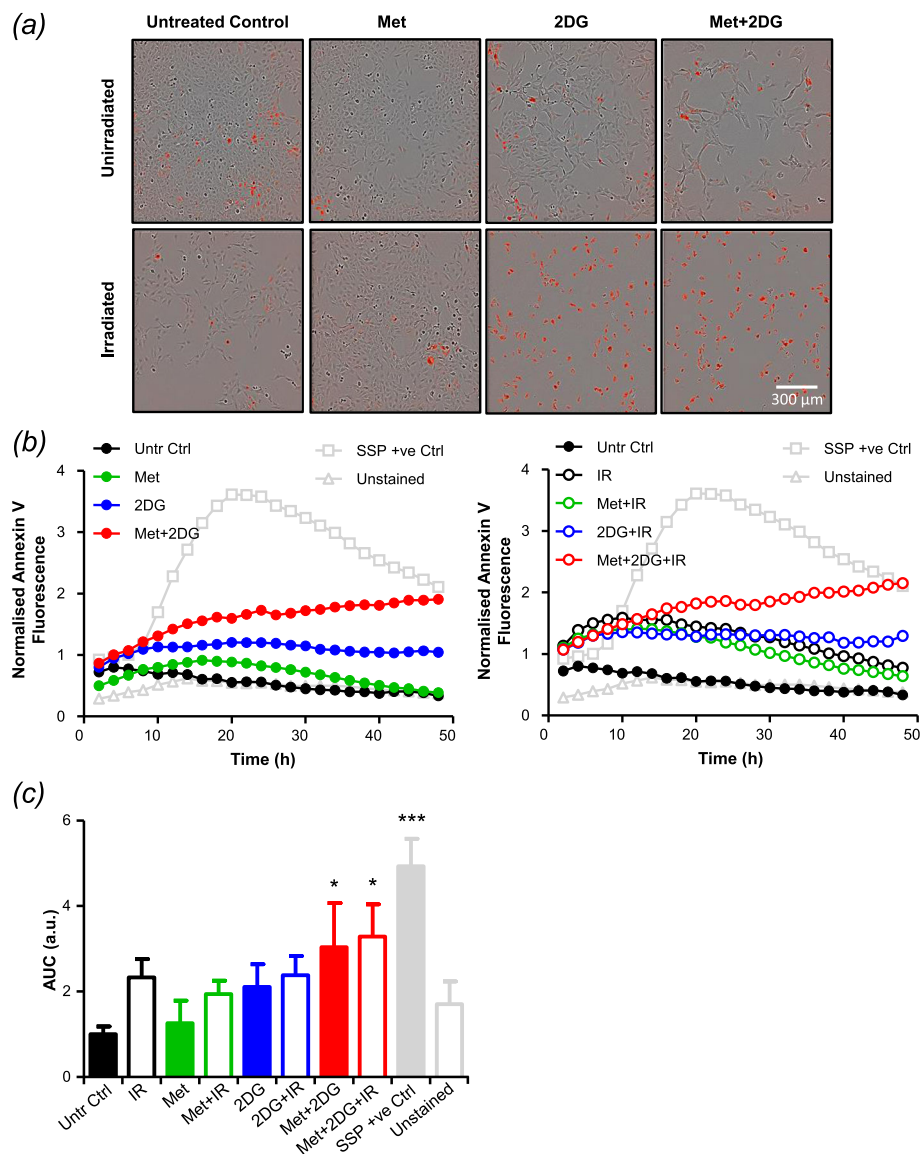


**Fig. 6** The effect of combination treatment on apoptotic frequency. UVW/NAT cells were treated with 2 Gy X-radiation (administered at the start of treatment), 1 mM metformin, or 1 mM 2DG as single agents or in combination for 48 h and were imaged every hour using the InCuCyte Zoom imaging system. Representative images taken after 48h treatment exposure are shown (a). Apoptotic frequency was determined following Annexin V staining. Annexin V-positive cells (displaying red fluorescence) were normalised to the total number of cells present (b) and the area under the curve (AUC) was calculated (c) to allow comparisons between each condition and the treatment controls (untreated control (Untr Ctrl), unstained negative control (unstained) and staurosporine positive control (SSP +ve)). Data are means  $\pm$  SEM from 3 separate experiments, each performed in sextuplet wells. \* $p < 0.05$ , \*\* $p < 0.01$  compared to untreated control cells (one-way ANOVA)

include CHLA-20 human neuroblastoma cells, which are non-*MYCN* amplified. Since CHLA-20 cells were unable to form clonogenic colonies, spheroid growth delay was used as a clinically relevant readout of radiosensitivity. In this cell line, dual treatment with 2-DG and metformin produced significantly greater radiosensitisation than either agent administered alone, supporting our findings in UVW/NAT cells and consistent with data derived from breast cancer [48, 50], prostate cancer [47] and paediatric glioma cells [49]. Our findings support a potential role for

*MYCN* amplification in treatment resistance of neuroblastoma cells that merits further investigation.

Interrogation of the cellular metabolome by mass spectrometric analysis demonstrated significant disruption of the glycolytic pathway and the electron transport chain (ETC) following exposure to 2-DG and metformin as single agents. We further showed that the greatest metabolite imbalance was observed following combination of 2-DG and metformin treatments. Even though this imbalance was not further exacerbated by irradiation, it set the scene for

enhanced radiosensitivity. Further investigations revealed that these large-scale metabolic imbalances ultimately culminated in reduced cellular energy production. These results were corroborated by real-time analysis of oxygen consumption rate using the Seahorse system, wherein triple combination therapy produced a substantial shift in bioenergetic profile from a highly energetic to a largely quiescent cellular phenotype. Additionally, we observed significantly reduced ATP production, glycolytic rate, and respiratory capacity following exposure to combination treatments. Similar analysis of biogenetic profiles proved useful during the characterisation of different histological subtypes of ovarian cancer, in which highly glycolytic cell subtypes exhibited greater susceptibility to 2-DG [58]. A key question is how do the metabolic imbalances detailed in this study relate to cell death following radiotherapy? Our data support a model in which (1) metabolic shifts from a highly energetic state to cellular quiescence prevent proliferation and (2) increased reliance on mitochondrial energy production following glycolytic inhibition increases production of reactive oxygen species (ROS), which enhances radiation-induced ROS production, thus increasing cytotoxicity. We hypothesise that inhibition of glycolysis by 2-DG causes a metabolic shift to oxidative phosphorylation (OXPHOS) in order to sustain ATP production, a compensatory mechanism that can be circumvented by adding metformin. Albeit by alternative methodologies, several other studies have also demonstrated reduced ATP content as a possible mechanism of additivity when 2-DG is combined with metformin [47, 49, 50].

Of course, the radiosensitising effect of 2-DG may not be solely due to inhibition of glycolysis. 2-DG is known to exert off-target effects as a mannose mimetic and can cause post-translational modifications such as N-linked glycosylation [59]. Indeed, N-linked glycosylation, in which an oligosaccharide is attached to a protein residue via its nitrogen atom, is a post-translational event analogous to poly(ADP-ribose)ation, whereby ADP-ribose moieties are attached to a target protein at the site of DNA damage. We have previously demonstrated the radiosensitising properties of the poly(ADP-ribose) polymerase-1 (PARP-1) inhibitors olaparib and rucaparib in neuroblastoma and glioma cells, where they act principally by preventing repair of radiation-induced damage [38]. Indeed, this radiation-induced poly(ADP-ribose)ation which would consume pools of NAD<sup>+</sup> and ADP, would occur synonymously with the ATP depletion following combined 2-DG/metformin treatment. Presumably, AMP supplies would be depleted in attempts to replenish ADP/ATP levels. This may be a possible explanation as to why we observed significant reductions in abundance of AMP, ADP, ATP and NAD<sup>+</sup> following combination therapy.

In addition to its well-documented effects on glucose metabolism, we also demonstrated that 2-DG treatment had

significant effects on purine and pyrimidine metabolism. Of note were the changes observed in ethanolamine phosphate and hypoxanthine, which are generated by carboxylation of serine and deamination of adenine, respectively. These metabolites were significantly increased by dual and triple combination therapies, but not by single agent treatments. Their increased abundance may reflect attempts to repair radiation-induced DNA damage, which require cells to increase de novo purine and pyrimidine synthesis, with input from serine and adenine, to synthesise the nucleotides required for DNA repair. Indeed, nucleotide metabolism has been implicated in oncogene-induced cellular senescence due to the roles of nucleotides in replication stress and the DNA damage response [60].

Flow cytometric analysis revealed that although 2-DG and metformin, as single agents, induced modest accumulation of cells in the G<sub>2</sub>/M phase of the cell cycle, maximum G<sub>2</sub>/M arrest was achieved by combining the two agents, as previously shown by others [47, 48]. Our data also demonstrated that this G<sub>2</sub>/M arrest could be further enhanced by combination with X-irradiation and, more importantly, that it persisted for at least 24 h after irradiation. This indicated that optimal scheduling of therapeutic modalities could maximise arrest in G<sub>2</sub>/M — the most radiosensitive phase of the cell cycle. Indeed, we went on to show that scheduling X-irradiation exposure 6 h before 2-DG/metformin treatment maximised G<sub>2</sub>/M arrest. However, this treatment schedule did not further enhance clonogenic cell kill compared to the other two schedules, which is why simultaneous combinations were used for the rest of the study. We predicted that the mechanism by which the 2-DG/metformin combination increased radiosensitivity entailed induction of apoptosis during prolonged G<sub>2</sub>/M accumulation of cells, as shown previously [47, 49, 50]. This hypothesis was supported by our Incucyte data which showed the frequency of Annexin V-stained UVW/NAT and CHLA-20 cells to be significantly enhanced following 2-DG/metformin treatment, compared to single agent administration.

Like most other *in vitro* studies investigating this drug combination [47–50], we observed cytotoxic activity of 2-DG and metformin only at higher drug concentrations than could be achieved clinically. In contrast, we observed potent radiosensitising effects of the combination with lower concentrations (1 mM). Clinically, the recommended dose of 2-DG is 63 mg/kg/day (75 μM<sup>1</sup>), which achieved maximum plasma concentrations in the region of 116 μg/ml (0.7 μM) [23], although higher doses may be tolerated in combination with radiation therapy. And while metformin is not usually given to diabetic patients at doses higher than 1500–2000 mg/day, which deliver plasma concentrations of 22–29 μM<sup>1</sup> [27], it should be noted that shorter treatment

<sup>1</sup>Assuming 80 kg average weight and 5.15 L average circulating blood volume.

regimens would be required in combination with radiotherapy, so it may be feasible to treat neuroblastoma patients with higher daily doses. Since both drugs are already clinically approved, exhibit favourable toxicity profiles and, as far as the authors are aware, have no documented maximum tolerated dose to date, we consider them to be promising therapeutic agents in combination with radiation therapy in paediatric patients.

## Conclusions

In summary, we show for the first time that the glycolytic inhibitor 2-DG enhances the radiosensitivity of human neuroblastoma and glioma cells *in vitro*. The radiosensitising effects of 2-DG were greatly enhanced by combination with the antidiabetic biguanide, metformin. Metabolomic analysis revealed this combination to elicit severe disruption of key glycolytic and mitochondrial metabolites, causing significant reductions in ATP generation. These results were supported by cellular bioenergetic profiling. Combination treatment induced G<sub>2</sub>/M arrest that persisted for at least 24 h post-irradiation, promoting apoptotic cell death in a significant proportion of cells. Our findings suggest that targeting cellular metabolism has potential to improve clinical outcomes by overcoming radioresistance in children with high-risk neuroblastoma.

## Abbreviations

2DG: 2-Deoxyglucose; AUC: Area under the curve; DEF<sub>50</sub>: Dose enhancement factor observed at the 50% kill level; DMEM: Dulbecco's modified Eagle medium; ECAR: Extracellular acidification rate; HILIC: Hydrophilic interaction liquid chromatography; IC<sub>50</sub>: 50% Inhibitory concentration; IR: Irradiated/irradiation; MIBG: Meta-iodobenzylguanidine; NAT: Noradrenaline transporter; OCR: Oxygen consumption rate; OXPHOS: Oxidative phosphorylation; PARP-1: Poly(ADP-ribose) polymerase-1; PiMP: Polyomics integrated Metabolomics Pipeline; SSP: Staurosporine; TCA: Tricarboxylic acid

## Supplementary Information

The online version contains supplementary material available at <https://doi.org/10.1186/s40170-021-00258-5>.

**Additional file 1: Supplementary Figure S1.** The effect of 2-DG and metformin on cell survival. **Supplementary Figure S2.** The radiosensitising effect of 2-DG and metformin as single agents. **Supplementary Figure S3.** The effect of combination treatment on glycolytic and mitochondrial metabolites. **Supplementary Figure S4.** Effects of 2-DG treatment on purine metabolism. **Supplementary Figure S5.** Effects of 2-DG treatment on pyrimidine metabolism. **Supplementary Figure S6.** The effect of combination treatment on mitochondrial respiration, glycolysis and cellular energy production. **Supplementary Figure S7.** The effect of combination treatment on mitochondrial respiration, glycolysis and cellular energy production. **Supplementary Figure S8.** The effect of 2-DG and metformin on the cell cycle. **Supplementary Figure S9.** The effect of combination treatment on apoptotic frequency.

## Acknowledgements

The authors would thank Lucie de Beauchamp and David Strachan for their help and assistance with the Seahorse Analyser and the IncuCyte Imaging System, respectively.

## Authors' contributions

DLN, RJM, CR and MNG designed the study. DLN, CR, DW, JCW, IV and KB developed the methodologies and collected the data. DLN, DW and IV analysed the data. DLN, AJC, MNG and CR wrote and revised the paper. RJM, AJC and MNG supervised the study. All authors approved the final paper.

## Funding

This work was funded by Children with Cancer UK (grant numbers 15-191 and 17-243) and a Wellcome Institutional Strategic Support Fund (ISSF) Feasibility Award. Dr. Mark N. Gaze is supported by the National Institute for Health Research University College London Hospitals Biomedical Research Centre and by the Radiation Research Unit at the Cancer Research UK City of London Centre Award (C7893/A28990).

## Availability of data and materials

The datasets used and/or analysed during the current study are available from the corresponding author on reasonable request.

## Declarations

### Ethics approval and consent to participate

Not applicable.

### Consent for publication

All authors consent to the publication of data reported in this manuscript.

### Competing interests

The authors declare that they have no competing interests.

### Author details

<sup>1</sup>Institute of Cancer Sciences, University of Glasgow, Glasgow G61 1QH, UK. <sup>2</sup>Present Address: Integrated Covid Hub North East (ICHNE) Innovation Laboratory, Newcastle upon Tyne Hospitals NHS Foundation Trust, Newcastle upon Tyne NE4 5BX, UK. <sup>3</sup>Present Address: School of Medicine, University of Dundee, Dundee DD1 4HN, UK. <sup>4</sup>Glasgow Polyomics Facility, University of Glasgow, Glasgow G61 1QH, UK. <sup>5</sup>Present Address: Institute of Pharmacy and Biomedical Sciences, University of Strathclyde, Glasgow G4 0RE, UK. <sup>6</sup>Present Address: School of Biological Sciences, University of Edinburgh, Edinburgh EH8 9XD, UK. <sup>7</sup>Department of Oncology, University College London Hospitals NHS Foundation Trust, London NW1 2BU, UK.

Received: 16 September 2020 Accepted: 13 April 2021

Published online: 19 May 2021

## References

- Gains J, Mandeville H, Cork N, Brock P, Gaze M. Ten challenges in the management of neuroblastoma. *Future Oncol*. 2012;8(7):839–58. <https://doi.org/10.2217/fon.12.70>.
- Matthay KK, Maris JM, Schleiermacher G, Nakagawara A, Mackall CL, Diller L, et al. Neuroblastoma. *Nat Rev Dis Primers*. 2016;2(1):16078. <https://doi.org/10.1038/nrdp.2016.78>.
- Pearson AD, Pinkerton CR, Lewis IJ, Imeson J, Ellershaw C, Machin D. High-dose rapid and standard induction chemotherapy for patients aged over 1 year with stage 4 neuroblastoma: a randomised trial. *Lancet Oncol*. 2008;9(3):247–56. [https://doi.org/10.1016/S1470-2045\(08\)70069-X](https://doi.org/10.1016/S1470-2045(08)70069-X).
- Holmes K, Pötschger U, Pearson ADJ, Sarnacki S, Cecchetto G, Gomez-Chacon J et al. Influence of surgical excision on the survival of patients with stage 4 high-risk neuroblastoma: a report from the HR-NBL1/SIOPEN study. *J Clin Oncol*. 2020;38(25):2902–15. <https://doi.org/10.1200/JCO.19.03117>.
- Ladenstein R, Pötschger U, Pearson ADJ, Brock P, Luksch R, Castel V, et al. Busulfan and melphalan versus carboplatin, etoposide, and melphalan as high-dose chemotherapy for high-risk neuroblastoma (HR-NBL1/SIOPEN): an international, randomised, multi-arm, open-label, phase 3 trial. *Lancet Oncol*. 2017;18(4):500–14. [https://doi.org/10.1016/S1470-2045\(17\)30070-0](https://doi.org/10.1016/S1470-2045(17)30070-0).
- Arumugam S, Manning-Cork NJ, Gains JE, Boterberg T, Gaze MN. The evidence for external beam radiotherapy in high-risk neuroblastoma of childhood: a systematic review. *Clin Oncol (R Coll Radiol)*. 2019;31(3):182–90. <https://doi.org/10.1016/j.clon.2018.11.031>.
- Ladenstein R, Pötschger U, Valteau-Couanet D, Luksch R, Castel V, Ash S et al. Investigation of the role of dinutuximab beta-based immunotherapy

- in the SIOPEN High-Risk Neuroblastoma 1 trial (HR-NBL1). *Cancers (Basel)*. 2020;12(2):309. <https://doi.org/10.3390/cancers12020309>.
8. Mairs RJ, Gaze MN, Barrett A. The uptake and retention of metaiodobenzylguanidine by the neuroblastoma cell line NB1-G. *Br J Cancer*. 1991;64(2):293–5. <https://doi.org/10.1038/bjc.1991.294>.
  9. Wilson JS, Gains JE, Moroz V, Wheatley K, Gaze MN. A systematic review of 131I-meta iodobenzylguanidine molecular radiotherapy for neuroblastoma. *Eur J Cancer*. 2014;50(4):801–15. <https://doi.org/10.1016/j.ejca.2013.11.016>.
  10. Berthold F, Spix C, Kaatsch P, Lampert F. Incidence, survival, and treatment of localized and metastatic neuroblastoma in Germany 1979–2015. *Paediatr Drugs*. 2017;19(6):577–93. <https://doi.org/10.1007/s40272-017-0251-3>.
  11. Pinto NR, Applebaum MA, Volchenboum SL, Matthay KK, London WB, Ambros PF, et al. Advances in risk classification and treatment strategies for neuroblastoma. *J Clin Oncol*. 2015;33(27):3008–17. <https://doi.org/10.1200/JCO.2014.59.4648>.
  12. Park JR, Kreissman SG, London WB, Naranjo A, Cohn SL, Hogarty MD, et al. Effect of tandem autologous stem cell transplant vs single transplant on event-free survival in patients with high-risk neuroblastoma: a randomized clinical trial. *JAMA*. 2019;322(8):746–55. <https://doi.org/10.1001/jama.2019.11642>.
  13. Gaze MN, Gains JE, Walker C, Bomanji JB. Optimization of molecular radiotherapy with [131I]-meta iodobenzylguanidine for high-risk neuroblastoma. *Q J Nucl Med Mol Imaging*. 2013;57(1):66–78.
  14. Mairs RJ, Boyd M. Preclinical assessment of strategies for enhancement of metaiodobenzylguanidine therapy of neuroendocrine tumors. *Semin Nucl Med*. 2011;41(5):334–44. <https://doi.org/10.1053/j.semnuclmed.2011.03.004>.
  15. Warburg O. *The metabolism of tumours*: Arnold Constable London, UK; 1930.
  16. Zhao Y, Butler EB, Tan M. Targeting cellular metabolism to improve cancer therapeutics. *Cell Death Dis*. 2013;4(3):e532. <https://doi.org/10.1038/cddis.2013.60>.
  17. El Mjiyyad N, Caro-Maldonado A, Ramirez-Peinado S, Munoz-Pinedo C. Sugar-free approaches to cancer cell killing. *Oncogene*. 2011;30(3):253–64. <https://doi.org/10.1038/ncr.2010.466>.
  18. Meijer TW, Kaanders JH, Span PN, Bussink J. Targeting hypoxia, HIF-1, and tumor glucose metabolism to improve radiotherapy efficacy. *Clin Cancer Res*. 2012;18(20):5585–94. <https://doi.org/10.1158/1078-0432.CCR-12-0858>.
  19. Slade RF, Hunt DA, Pochet MM, Venema VJ, Hennigar RA. Characterization and inhibition of fatty acid synthase in pediatric tumor cell lines. *Anticancer Res*. 2003;23(2B):1235–43.
  20. Zirath H, Frenzel A, Olynyk G, Segerstrom L, Westermark UK, Larsson K, et al. MYC inhibition induces metabolic changes leading to accumulation of lipid droplets in tumor cells. *Proc Natl Acad Sci U S A*. 2013;110(25):10258–63. <https://doi.org/10.1073/pnas.1222404110>.
  21. Storz P. Reactive oxygen species in tumor progression. *Front Biosci*. 2005;10(2):1881–96. <https://doi.org/10.2741/1667>.
  22. Lin X, Zhang F, Bradbury CM, Kaushal A, Li L, Spitz DR, et al. 2-Deoxy-D-glucose-induced cytotoxicity and radiosensitization in tumor cells is mediated via disruptions in thiol metabolism. *Cancer Res*. 2003;63(12):3413–7.
  23. Raez LE, Papadopoulos K, Ricard AD, Chiorean EG, Dipaola RS, Stein MN, et al. A phase I dose-escalation trial of 2-deoxy-D-glucose alone or combined with docetaxel in patients with advanced solid tumors. *Cancer Chemother Pharmacol*. 2013;71(2):523–30. <https://doi.org/10.1007/s00280-012-2045-1>.
  24. Shaw RJ, Lamia KA, Vasquez D, Koo SH, Bardeesy N, Depinho RA, et al. The kinase LKB1 mediates glucose homeostasis in liver and therapeutic effects of metformin. *Science*. 2005;310(5754):1642–6. <https://doi.org/10.1126/science.1120781>.
  25. El-Mir MY, Nogueira V, Fontaine E, Averet N, Rigoulet M, Leverve X. Dimethylbiguanide inhibits cell respiration via an indirect effect targeted on the respiratory chain complex I. *J Biol Chem*. 2000;275(1):223–8. <https://doi.org/10.1074/jbc.275.1.223>.
  26. Owen MR, Doran E, Halestrap AP. Evidence that metformin exerts its anti-diabetic effects through inhibition of complex 1 of the mitochondrial respiratory chain. *Biochem J*. 2000;348(Pt 3):607–14. <https://doi.org/10.1042/bj3480607>.
  27. Pollak M. Potential applications for biguanides in oncology. *J Clin Invest*. 2013;123(9):3693–700. <https://doi.org/10.1172/JCI67232>.
  28. Jiralerspong S, Palla SL, Giordano SH, Meric-Bernstam F, Liedtke C, Barnett CM, et al. Metformin and pathologic complete responses to neoadjuvant chemotherapy in diabetic patients with breast cancer. *J Clin Oncol*. 2009;27(20):3297–302. <https://doi.org/10.1200/JCO.2009.19.6410>.
  29. Libby G, Donnelly LA, Donnan PT, Alessi DR, Morris AD, Evans JM. New users of metformin are at low risk of incident cancer: a cohort study among people with type 2 diabetes. *Diabetes Care*. 2009;32(9):1620–5. <https://doi.org/10.2337/dc08-2175>.
  30. Margel D, Urbach DR, Lipscombe LL, Bell CM, Kulkarni G, Austin PC, et al. Metformin use and all-cause and prostate cancer-specific mortality among men with diabetes. *J Clin Oncol*. 2013;31(25):3069–75. <https://doi.org/10.1200/JCO.2012.46.7043>.
  31. Fasih A, Elbaz HA, Huttemann M, Konski AA, Zielske SP. Radiosensitization of pancreatic cancer cells by metformin through the AMPK pathway. *Radiat Res*. 2014;182(1):50–9. <https://doi.org/10.1667/RR13568.1>.
  32. Liu J, Hou M, Yuan T, Yi G, Zhang S, Shao X, et al. Enhanced cytotoxic effect of low doses of metformin combined with ionizing radiation on hepatoma cells via ATP deprivation and inhibition of DNA repair. *Oncol Rep*. 2012;28(4):1406–12. <https://doi.org/10.3892/or.2012.1932>.
  33. Singh D, Banerji AK, Dwarakanath BS, Tripathi RP, Gupta JP, Mathew TL, et al. Optimizing cancer radiotherapy with 2-deoxy-D-glucose dose escalation studies in patients with glioblastoma multiforme. *Strahlenther Onkol*. 2005;181(8):507–14. <https://doi.org/10.1007/s00066-005-1320-z>.
  34. Zhang Y, Storr SJ, Johnson K, Green AR, Rakha EA, Ellis IO, et al. Involvement of metformin and AMPK in the radioresponse and prognosis of luminal versus basal-like breast cancer treated with radiotherapy. *Oncotarget*. 2014;5(24):12936–49. <https://doi.org/10.18632/oncotarget.2683>.
  35. Chuang JH, Chou MH, Tai MH, Lin TK, Liou CW, Chen T, et al. 2-Deoxyglucose treatment complements the cisplatin- or BH3-only mimetic-induced suppression of neuroblastoma cell growth. *Int J Biochem Cell Biol*. 2013;45(5):944–51. <https://doi.org/10.1016/j.biocel.2013.01.019>.
  36. Esteva FJ, Moulder SL, Gonzalez-Angulo AM, Ensor J, Murray JL, Green MC, et al. Phase I trial of exemestane in combination with metformin and risoglitazone in nondiabetic obese postmenopausal women with hormone receptor-positive metastatic breast cancer. *Cancer Chemother Pharmacol*. 2013;71(1):63–72. <https://doi.org/10.1007/s00280-012-1977-9>.
  37. Boyd M, Cunningham SH, Brown MM, Mairs RJ, Wheldon TE. Noradrenaline transporter gene transfer for radiation cell kill by <sup>131</sup>I meta-iodobenzylguanidine. *Gene Ther*. 1999;6(6):1147–52. <https://doi.org/10.1038/sj.gt.3300905>.
  38. Nile DL, Rae C, Hyndman IJ, Gaze MN, Mairs RJ. An evaluation in vitro of PARP-1 inhibitors, rucaparib and olaparib, as radiosensitisers for the treatment of neuroblastoma. *BMC Cancer*. 2016;16(1):621. <https://doi.org/10.1186/s12885-016-2656-8>.
  39. Rae C, Haberkorn U, Babich JW, Mairs RJ. Inhibition of fatty acid synthase sensitizes prostate cancer cells to radiotherapy. *Radiat Res*. 2015;184(5):482–93. <https://doi.org/10.1667/RR14173.1>.
  40. Tesson M, Vasan R, Hock A, Nixon C, Rae C, Gaze M, et al. An evaluation in vitro of the efficacy of nutlin-3 and topotecan in combination with (177)Lu-DOTATATE for the treatment of neuroblastoma. *Oncotarget*. 2018;9(49):29082–96. <https://doi.org/10.18632/oncotarget.25607>.
  41. Neshasteh-Riz A, Angerson WJ, Reeves JR, Smith G, Rampling R, Mairs RJ. Incorporation of iododeoxyuridine in multicellular glioma spheroids: implications for DNA-targeted radiotherapy using Auger electron emitters. *Br J Cancer*. 1997;75(4):493–9. <https://doi.org/10.1038/bjc.1997.86>.
  42. Tautenhahn R, Bottcher C, Neumann S. Highly sensitive feature detection for high resolution LC/MS. *BMC Bioinformatics*. 2008;9(1):504. <https://doi.org/10.1186/1471-2105-9-504>.
  43. Scheltema RA, Jankevics A, Jansen RC, Swertz MA, Breitling R. PeakML/mzMatch: a file format, Java library, R library, and tool-chain for mass spectrometry data analysis. *Anal Chem*. 2011;83(7):2786–93. <https://doi.org/10.1021/ac2000994>.
  44. Gloaguen Y, Morton F, Daly R, Gurden R, Rogers S, Wandy J, et al. PIMP my metabolome: an integrated, web-based tool for LC-MS metabolomics data. *Bioinformatics*. 2017;33(24):4007–9. <https://doi.org/10.1093/bioinformatics/btx499>.
  45. Vande Voorde J, Ackermann T, Pfetzer N, Sumpton D, Mackay G, Kalna G, et al. Improving the metabolic fidelity of cancer models with a physiological cell culture medium. *Sci Adv*. 2019;5(1):eaau7314.
  46. Nile DL, Brown AE, Kumaheri MA, Blair HR, Heggie A, Miwa S, et al. Age-related mitochondrial DNA depletion and the impact on pancreatic Beta cell function. *Plos One*. 2014;9(12):e115433. <https://doi.org/10.1371/journal.pone.0115433>.
  47. Ben Sahara I, Laurent K, Giuliano S, Larbret F, Ponzio G, Gounon P, et al. Targeting cancer cell metabolism: the combination of metformin and 2-deoxyglucose induces p53-dependent apoptosis in prostate cancer cells.

- Cancer Res. 2010;70(6):2465–75. <https://doi.org/10.1158/0008-5472.CAN-09-2782>.
48. Bizjak M, Malavasic P, Dolinar K, Pohar J, Pirkmajer S, Pavlin M. Combined treatment with metformin and 2-deoxy glucose induces detachment of viable MDA-MB-231 breast cancer cells in vitro. *Sci Rep*. 2017;7(1):1761. <https://doi.org/10.1038/s41598-017-01801-5>.
  49. Levesley J, Steele L, Taylor C, Sinha P, Lawler SE. ABT-263 enhances sensitivity to metformin and 2-deoxyglucose in pediatric glioma by promoting apoptotic cell death. *Plos One*. 2013;8(5):e64051. <https://doi.org/10.1371/journal.pone.0064051>.
  50. Chatterjee S, Thaker N, De A. Combined 2-deoxy glucose and metformin improves therapeutic efficacy of sodium-iodide symporter-mediated targeted radioiodine therapy in breast cancer cells. *Breast Cancer (Dove Med Press)*. 2015;7:251–65.
  51. McCluskey AG, Mairs RJ, Tesson M, Pimlott SL, Babich JW, Gaze MN, et al. Inhibition of poly(ADP-Ribose) polymerase enhances the toxicity of <sup>131</sup>I-metaiodobenzylguanidine/topotecan combination therapy to cells and xenografts that express the noradrenaline transporter. *J Nucl Med*. 2012; 53(7):1146–54. <https://doi.org/10.2967/jnumed.111.095943>.
  52. Pawlik TM, Keyomarsi K. Role of cell cycle in mediating sensitivity to radiotherapy. *Int J Radiat Oncol Biol Phys*. 2004;59(4):928–42. <https://doi.org/10.1016/j.ijrobp.2004.03.005>.
  53. Matthay KK, Yanik G, Messina J, Quach A, Huberty J, Cheng SC, et al. Phase II study on the effect of disease sites, age, and prior therapy on response to iodine-131-metaiodobenzylguanidine therapy in refractory neuroblastoma. *J Clin Oncol*. 2007;25(9):1054–60. <https://doi.org/10.1200/JCO.2006.09.3484>.
  54. Ruiz-Perez MV, Medina MA, Urdiales JL, Keinanen TA, Sanchez-Jimenez F. Polyamine metabolism is sensitive to glycolysis inhibition in human neuroblastoma cells. *J Biol Chem*. 2015;290(10):6106–19. <https://doi.org/10.1074/jbc.M114.619197>.
  55. Tweddle DA, Malcolm AJ, Bown N, Pearson AD, Lunec J. Evidence for the development of p53 mutations after cytotoxic therapy in a neuroblastoma cell line. *Cancer Res*. 2001;61(1):8–13.
  56. Keshelava N, Seeger RC, Groshen S, Reynolds CP. Drug resistance patterns of human neuroblastoma cell lines derived from patients at different phases of therapy. *Cancer Res*. 1998;58(23):5396–405.
  57. Brodeur GM, Seeger RC, Schwab M, Varmus HE, Bishop JM. Amplification of N-myc in untreated human neuroblastomas correlates with advanced disease stage. *Science*. 1984;224(4653):1121–4. <https://doi.org/10.1126/science.6719137>.
  58. Dier U, Shin DH, Hemachandra LP, Uusitalo LM, Hempel N. Bioenergetic analysis of ovarian cancer cell lines: profiling of histological subtypes and identification of a mitochondria-defective cell line. *Plos One*. 2014;9(5): e98479. <https://doi.org/10.1371/journal.pone.0098479>.
  59. Xi H, Kurtoglu M, Lampidis TJ. The wonders of 2-deoxy-D-glucose. *IUBMB Life*. 2014;66(2):110–21. <https://doi.org/10.1002/iub.1251>.
  60. Aird KM, Zhang R. Nucleotide metabolism, oncogene-induced senescence and cancer. *Cancer Lett*. 2015;356(2 Pt A):204–10.

## Publisher's Note

Springer Nature remains neutral with regard to jurisdictional claims in published maps and institutional affiliations.

**Ready to submit your research? Choose BMC and benefit from:**

- fast, convenient online submission
- thorough peer review by experienced researchers in your field
- rapid publication on acceptance
- support for research data, including large and complex data types
- gold Open Access which fosters wider collaboration and increased citations
- maximum visibility for your research: over 100M website views per year

**At BMC, research is always in progress.**

Learn more [biomedcentral.com/submissions](https://biomedcentral.com/submissions)

